

Tests of an electromagnetic calorimeter prototype for the PEBS experiment

Aurelio Bay^b, Guenther Dissertori^c, Alex Gong^a, Oliver Grimm^c, Guido Haefeli^b, Liang Li^a, Changxing Lin^a, Jean-Baptiste Mosset^{*b}, Werner Luster^c, Tatsuya Nakada^b, Lesya Shchutska^b, Paola Solevi^c, Fabien Zehr^{*b}

^aTsinghua University, Beijing, China

^bLaboratoire de Physique des Hautes Energies, EPFL, CH-1015 Lausanne, Switzerland

^cInstitute for Particle Physics, ETH Zurich, CH-8093 Zurich, Switzerland

Abstract

The positron excess in cosmic rays recently reported by PAMELA has raised considerable interest. Possible interpretations are the presence of a nearby pulsar or the annihilation of exotic dark matter particles. The large acceptance PEBS detector (Positron Electron Balloon Spectrometer) is proposed to provide measurements of the electron + positron flux up to 2 TeV and positron fraction up to 600 GeV with an unprecedented statistical quality of the data. Together with a scintillating fibre tracker and a transition radiation detector, PEBS features an electromagnetic calorimeter consisting of sandwiched scintillating layers between W absorber plates. Each layer is made of a series of scintillating bars with a small cross section ($7.75 \times 3 \text{ mm}^2$). Each scintillating bar is optically isolated and equipped with wavelength shifting fibres readout by silicon photomultipliers. Its very good energy resolution is essential for a good proton background rejection (10^3) from the shower profile. A small scale ECAL prototype (with Pb absorber) has been built and tested at CERN in November 2009. Results on the shower profile measurements and comparison with the simulation are presented, together with the characterization of the MPPCs used in this ECAL prototype.

Key words: Electromagnetic calorimeter, SiPM, MPPC

1. Introduction

Recent results on the positron fraction in cosmic rays reported by PAMELA [1] and on the $e^+ + e^-$ total flux by FERMI [2] and HESS [3] have raised considerable interest. Possible explanations are the presence of a nearby pulsar, an exploding Wolf-Rayet star or the first observational signature of dark matter particles annihilation or decay.

In order to put more constraints on such models, the balloon-borne detector PEBS (Positron Electron Balloon Spectrometer [4]) has been proposed. It will measure the e^+ and e^- fluxes in the upper atmosphere (40 km) with an unprecedented precision. The spectrometer comprises a scintillating fibre tracker, a transition radiation detector and an electromagnetic calorimeter (ECAL). Its very good proton rejection of 10^6 and 10^5 at 100 GeV and 1 TeV respectively (where $N_p/N_{e^-} = 10^4$ and 10^5 respectively) permits a measurement of the total electron + positron flux up to ~ 2 TeV. In addition, the use of a 0.34 T permanent magnet will allow to separate positrons from electrons and thus determine the positron fraction up to ~ 600 GeV. This last value might be increased to ~ 2 TeV in a proposed upgrade, PEBS 2, using a 0.8 T superconducting magnet. The ECAL itself will contribute with a factor of 10^3 to the total proton rejection by measuring the shower profiles. It consists of 21 layers of 3 mm thick W absorber plates ($11.25 X_0$) sandwiched between scintillator layers. Each layer is made of 108

$7.75 \times 3 \times 837 \text{ mm}^3$ scintillating bars. Each bar has an embedded WaveLength Shifting (WLS) fibre that collects the light, read out by a Multi Pixel Photon Counter (MPPC). The bars are optically isolated from each other.

2. MPPC characterization

MPPCs have been chosen as photodetectors for the ECAL, since they are compact, insensitive to magnetic fields and they only need a small bias voltage of about 70 V. The selected MPPC (fig. 1) is produced by Hamamatsu photonics [5]. It is very similar to the standard S10362-11-025C MPPC, but the shape of the casing and the active area of $1.4 \times 1.4 \text{ mm}^2$ has been adapted for the requirements of the ECAL design. The pixel size is $25 \times 25 \mu\text{m}^2$. The MPPCs are mounted onto a PCB and protected with a $250 \mu\text{m}$ thick epoxy layer.

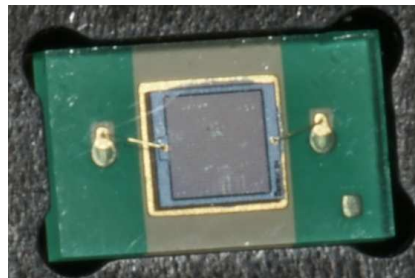


Figure 1: MPPC used in the ECAL prototype.

*Corresponding authors



Figure 2: Front-end electronics to read out the MPPCs.



Figure 3: ADC board.

2.1. Materials and Methods

Light Emitting Diodes (LED) which produce 10 ns long light pulses are used as light source. The light is transmitted through a diffusing glass and illuminates homogeneously a rotating mirror which has two stable positions and can reflect the light either on a calibrated PMT, or on the MPPC being tested. A set of LEDs emitting at different wavelengths is used to determine the Photon Detection Efficiency (PDE) in the VIS-UV range. Two Peltier elements allow to control the MPPC temperature between -10°C and 30°C with an accuracy of $\pm 0.1^{\circ}\text{C}$. The readout electronics is based on the SPIROC chip [6] (fig. 2), a 36-channel amplifier ASIC with adjustable gain and shaping time. Combined with our MPPC, its dynamic range is 2000 photons. The analog values of the 36 pulse heights are multiplexed out by the SPIROC and digitized by the EPFL-designed USB-Board (fig. 3) using a 12 bit ADC.

Figure 4 shows a typical distribution of the MPPC when it is illuminated with weak light pulses. Peaks corresponding to 1,2,3 or more photon peaks are well separated, allowing a characterization of the MPPC. The gain of the MPPC is determined from the number of ADC counts between the pedestal and the single photon peak. The PDE is given by the ratio between the mean number of photoelectrons n_{pe} measured by the MPPC and the mean number of photons reaching the MPPC which is measured by a calibrated PMT. Assuming the number of photoelectrons follows a Poisson statistics, n_{pe} can be determined from the number of events in the pedestal. The probability of crosstalk C is determined by comparing the number of true single photon events estimated from the number of pedestal events assuming the Poisson distribution, with the observed number of single photon events.

2.2. Results and discussion

Gain, PDE and crosstalk were measured as a function of the temperature for 10 MPPC. All MPPC characteristics only depend on the over voltage ΔU , which is the difference between the bias voltage and the breakdown voltage. This can be observed on figures 5 and 6 that show gain and PDE as a function of the over voltage at four different temperatures, for a given MPPC. The breakdown voltage has been determined as a function of the temperature (fig. 7). Its average temperature coefficient amounts to 55 mV/K. Figure 8 shows the PDE averaged over 10 MPPCs as a function of the wavelength, for an overvoltage of 3 V at 20°C . The peak sensitivity wavelength matches very well the emission peak of the WLS fibre (476 nm). Figures

9, 10, 11 show the gain, the photon detection efficiency and the crosstalk measured as a function of the over voltage at 20°C , for 100 MPPCs, respectively.

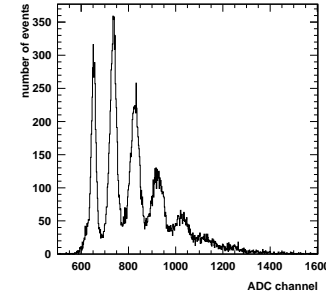


Figure 4: ADC distribution of MPPC output.

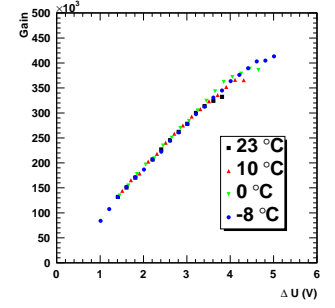


Figure 5: Gain versus over voltage at four different temperatures, for a given MPPC.

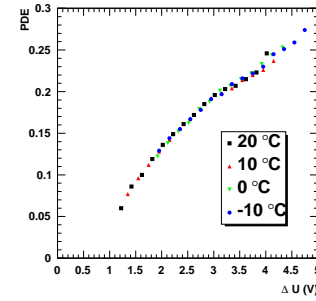


Figure 6: PDE versus over voltage at four different temperatures, for a given MPPC.

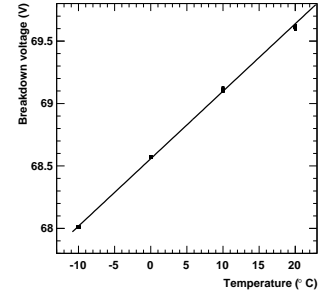


Figure 7: Breakdown voltage as a function of the temperature for a given MPPC.

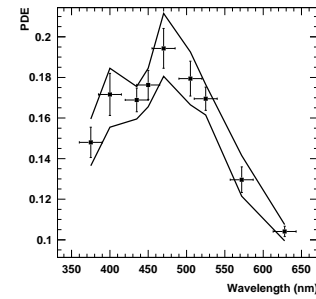


Figure 8: Average PDE with RMS errors versus illumination wavelength. Minimum and maximum PDE are bounded by the curves.

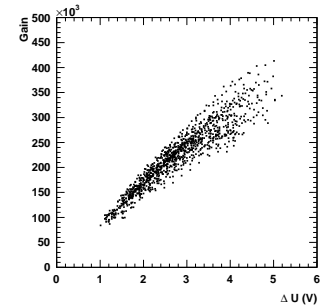


Figure 9: Gain versus over voltage, for 100 MPPCs.

2.3. Conclusion

The main results are given in Table 1. We have tested 100 MPPCs. No defect has been observed. Their characteristics are in good agreement with the datasheet and the device-by-device variation is small.

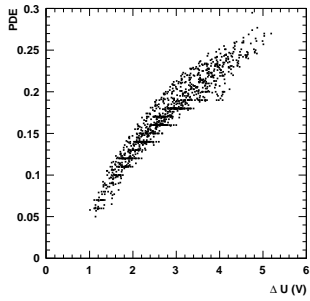


Figure 10: Photon detection efficiency versus over voltage at a wavelength of 470 nm, for 100 MPPCs.

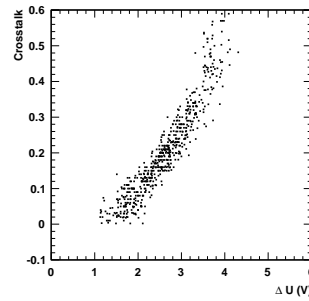


Figure 11: Crosstalk versus over voltage, for 100 MPPCs.

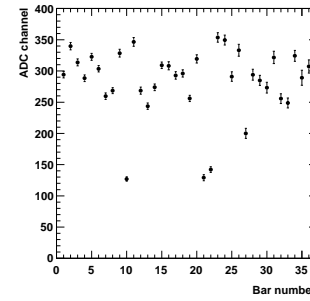


Figure 12: Muon response for all 36 channels at the non-filtered side.

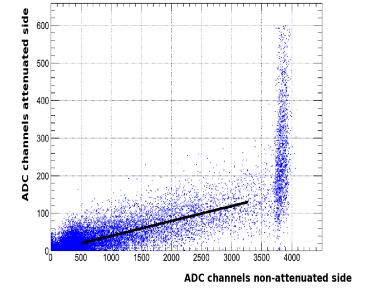


Figure 13: ADC readout for filtered vs non-filtered sides.

Gain ($U=72.4$ V)	$(2.25 \pm 0.10 \pm 0.11) \times 10^5$
PDE ($\lambda=470$ nm, $U=72.4$ V)	$(19.4 \pm 1.0 \pm 1.2) \%$
Crosstalk ($U=72.4$ V)	$(20 \pm 3 \pm 3) \%$
Breakdown voltage (U_b)	$(69.74 \pm 0.11 \pm 0.05)$ V
dU_b/dT	$(55 \pm 3 \pm 1)$ mV/ $^\circ$ C

Table 1: Main MPPC characteristics at 20 $^\circ$ C. The first error is the RMS and the second one the systematic uncertainty.

3. Testbeam at CERN

3.1. Prototype design

In order to test the PEBS calorimeter technology, a small scale ECAL prototype has been build. It is made of three scintillating layers using EJ-200 from Eljen Technologies, each layer comprising three $3 \times 7.35 \times 837$ mm³ bars. The bars have 1 mm diameter embedded WLS fibres from Kuraray (Y11(200)) in 1.1 mm deep and wide grooves. The fibres are glued with BC-600 optical cement and the assemblies are painted with BC-620 TiO₂ painting. Three Pb plates, 5 mm thick each, sandwiched between two 0.5 mm stainless steel sheets have been used as absorber corresponding to a total of $3.2 X_0$. The fibres are read out by MPPCs operated at an over voltage of 2.5 V. In order to cover the dynamic range while maintaining the desired resolution, both fibre ends are readout, one using a light attenuator made of aluminized Mylar, providing an attenuation factor of ~ 12 .

The detector has been tested at the CERN proton-synchrotron together with a tracker prototype built by RTWH Aachen [7] with 1 to 6 GeV electrons.

3.2. Results

The calibration of the prototype was performed with 4 GeV muons. The response at the non-filtered side for all 36 channels is shown in figure 12. It is ~ 300 ADC counts, similar for all 36 channels, corresponding to ~ 20 firing MPPC pixels (on average 17 primary photons and 3 crosstalk). Four fibres have been damaged during the gluing and have a smaller signal. Due to the low amplitude of the muon signals, the filtered side can't be calibrated in the same way. Therefore, the attenuated vs the non-attenuated response was plotted for each channel (fig. 13). The slope yields the calibration of the filtered side (fig. 14).

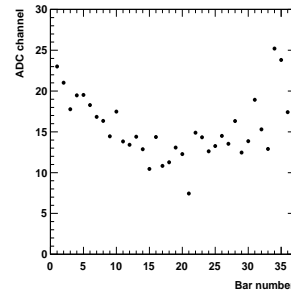


Figure 14: MIP response for all 36 channels at the filtered side. The signal is smaller in the center of the prototype due to the filter small inhomogeneity.

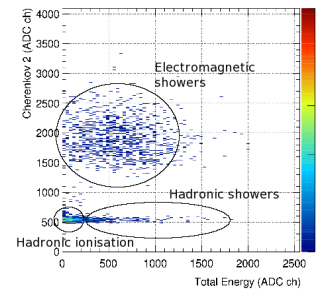


Figure 15: Second Čerenkov readout vs energy deposited in the ECAL.

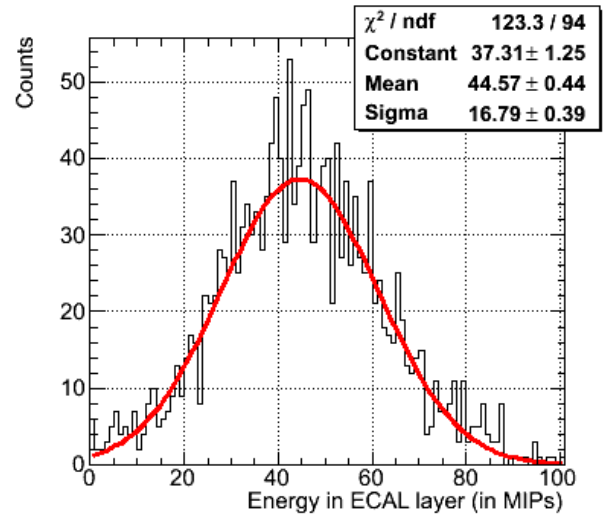


Figure 16: Total energy deposition in one ECAL layer for 4 GeV electrons at the shower maximum.

Electrons are selected by using two Čerenkov threshold detectors (fig. 15). Background from protons or pions is removed by using tracker information: for each electron candidate in the ECAL, a corresponding (single) track has to be present in the tracker. The total electron energy deposited in the ECAL is determined by a cluster algorithm that looks for the scintillating bar with the largest signal in each layer and recursively looks

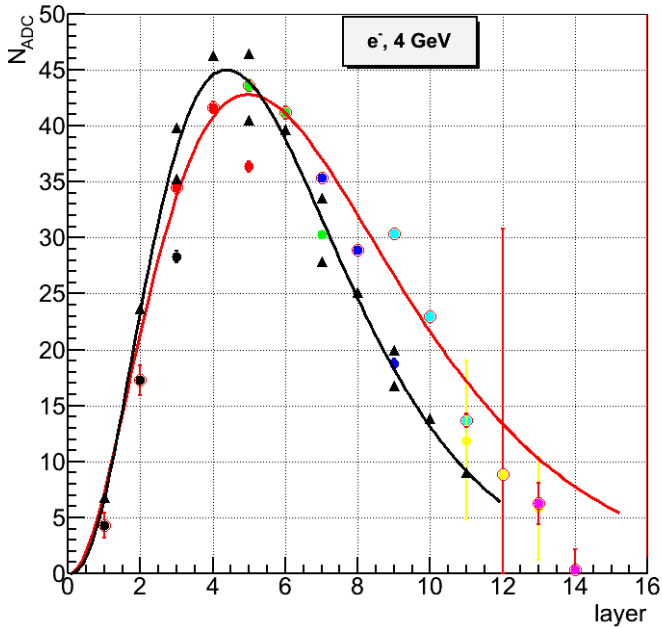


Figure 17: Shower profile for 4 GeV electrons in the ECAL (circles) compared with Monte Carlo (triangles). Each set of three points from the same color corresponds to a different lead thickness in front of the calorimeter (see text).

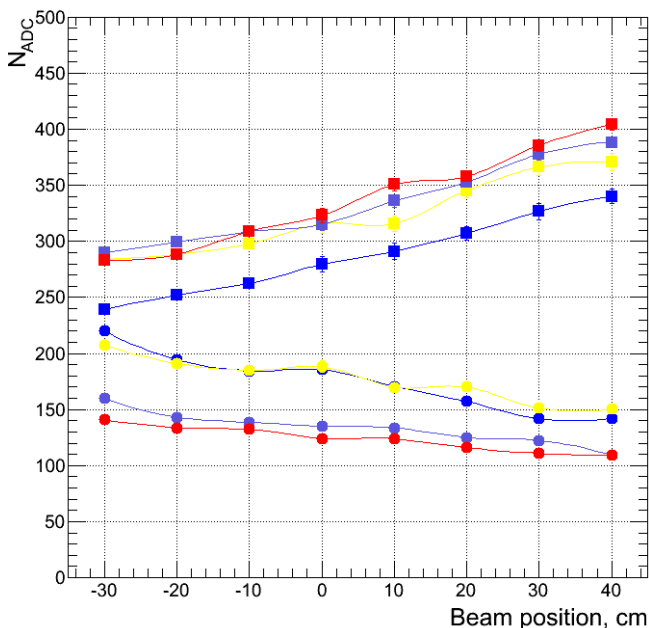


Figure 18: Total ECAL readout as a function of the beam position at non-attenuated (squares) and attenuated sides (circles, scaled 10x) for four different channels.

for neighbours with a signal above 0.2 MIPs. Finally, showers at the very edge of the ECAL prototype have an important energy leak and are discarded.

Using additional lead plates (10-60 mm) in front of the ECAL prototype, the shower profile was sampled up to 14 radiation length (fig. 17). Each set of three points of the same color in fig. 17 corresponds to the mean of Gaussian fits to the total energy deposited in each of the three layers (fig. 16). Different

sets belong to different lead thicknesses in front of the prototype. The results are compared with a dedicated Monte Carlo analysis and show a good agreement at 4 GeV. At this energy, the shower is almost fully contained within the first 14 absorber layers. The points have been fitted by the formula

$$\frac{dE}{dt} = E_0 b \frac{(bt)^{a-1} e^{-bt}}{\Gamma(a)}$$

where E_0 is the total shower energy (in MIPs), a and b are parameters that describe the scale and the maximum of the shower respectively and $t = z/X_0$ where z is the coordinate along the shower axis [8]. Let's note that, for each set of three points, the third one is systematically lower than expected. This is due to backscattering on the next Pb absorber layer, enhancing the signal for all but the last scintillating layer. In addition, we have measured the light yield of 12 GeV protons and pions as a function of the horizontal beam position for each channel. The results are plotted in fig. 18. The difference between the filtered and the non-filtered sides is about 20%, showing a small light attenuation in the fibre.

4. Conclusion and Outlook

An electromagnetic calorimeter prototype for the PEBS detector using Pb absorber plates, scintillating bars with embedded WLS filters, MPPC readout and dedicated electronics readout has been successfully tested at the CERN PS T9 line. It has a good response to MIPs at the non-filtered side, uniform response for the 36 channels at both filtered and non-filtered sides. It allows to measure the full electromagnetic shower profile and has a small dependence on the beam position along the scintillating bar. A new calorimeter prototype using tungsten instead of lead and the same scintillating bars and MPPCs is planned to be tested at CERN SPS in 2010. While the absorber scintillator assemblies are much shorter, it will feature up to 15 absorber layers, corresponding to 12.8 X_0 and improved readout electronics.

References

- [1] O. Adriani *et al.*, "Observation of an anomalous positron abundance in the cosmic radiation", *Nature*, 458, 2009.
- [2] A. Abdo *et al.*, "Measurement of the Cosmic Ray $e+$ plus $e-$ spectrum from 20 GeV to 1 TeV with the Fermi Large Area Telescope", *Phys. Rev. Lett.* 102 2009.
- [3] F. Aharonian *et al.*, "Energy Spectrum of Cosmic-Ray Electrons at TeV Energies", *Phys. Rev. Lett.* 101 2008.
- [4] P. von Doetinchem, H. Gast, T. Kirn, G. R. Yearwood and S. Schael, "PEBS - Positron Electron Balloon Spectrometer", *Nucl. Instr. Meth.*, A581, pp. 151-155, 2007.
- [5] Hamamatsu Photonics, K.K., Japan <http://sales.hamamatsu.com/>
- [6] M. Bouchel *et al.*, "SPIROC (SiPM Integrated Read-Out Chip): Dedicated very front-end electronics for an ILC prototype hadronic calorimeter with SiPM read-out", *Conf. Rec. IEEE Nucl. Sci. Symp.*, 2007.
- [7] G. Roper *et al.*, "The development of a high-resolution scintillating fiber tracker with silicon photomultiplier array readout", Proceeding of the 10th Vienna conference on instrumentation, to be published in *Nucl. Instr. Meth. A*, 2010.
- [8] E. Longo and I. Sestili, "Monte Carlo calculation of photon-initiated electromagnetic showers in lead glass", *Nucl. Instr. Meth.*, 128, 1975.